ELSEVIER

Catalysis Today 67 (2001) 403–409

CATALYSIS TODAY

www.elsevier.com/locate/cattod

Solid state chemistry of bulk mixed metal oxide catalysts for the selective oxidation of propane to acrylic acid

S.A. Holmes [a], J. Al-Saeedi [a], V.V. Guliants [a,*], P. Boolchand [b], D. Georgiev [b], U. Hackler [c], E. Sobkow [c]

[a] *Department of Chemical Engineering, University of Cincinnati, Cincinnati, OH 45221-0171, USA*
[b] *Department of Electrical Engineering, University of Cincinnati, Cincinnati, OH 45221-0030, USA*
[c] *Chemspeed Ltd, Rheinstrasse 32, CH-4302 Augst, Switzerland*

Abstract

Syntheses of Mo–V–Sb–Nb–O bulk materials, which are candidate catalyst systems for the selective oxidation of propane to acrolein and acrylic acid, were made using soluble precursor materials. The products were characterized by X-ray powder diffraction and Raman spectroscopic studies. The objectives of this work were to explore the utility of liquid phase automated synthesis for the preparation of bulk mixed metal oxides, and the identification of the oxide phases present in the system. This is the first published study of the phase composition for these materials. After calcination of these bulk oxides under flowing nitrogen at 600°C, and using stoichiometric ratios of Mo–V–Sb–Nb (1:1:0.4:0.4) and Mo–V–Sb–Nb (3.3:1:0.4:0.4) it was demonstrated that a mixture of phases were obtained for the syntheses. X-ray powder diffraction studies distinguished $SbVO_4$, $Mo_6V_9O_{40}$, MoO_3, and a niobium-stabilized defect phase of a vanadium-rich molybdate, $Mo_{0.61–0.77}V_{0.31–0.19}Nb_{0.08–0.04}O_x$, as the major phases present. Complementary data were provided by the Raman spectroscopic studies, which illustrated the heterogeneity of the phases present in the mixture. Raman also indicated bands attributable to the presence of phases containing terminal M=O bonds as well as M–O–M polycrystalline phases. Previous studies on this system have identified $SbVO_4$ and niobium-stabilized vanadium molybdate species as the active phases necessary for the selective oxidation of alkanes.

Keywords: Propane; Partial oxidation; Mixed metal oxides; Combinatorial

1. Introduction

Both economic and environmental concerns favor the use of alkane feedstocks over that of olefins. The use of mixed metal oxides for the oxidative dehydrogenation of olefins is already well established, with highly selective processes for the production of butadiene, isoprene and acrolein reported almost 40 years ago [1]. However, the current abundance and low cost of alkane feed-stocks has generated much recent interest in the oxidative catalytic conversion of alkanes to olefins, oxygenates, and nitriles in both the petroleum and petrochemical industries. Research has shown that the mixed Mo–V–Nb oxides [1,2] and Sb–V–Al oxides [3] are catalytically active for the oxidative dehydrogenation/selective oxidation of ethane and for propane ammoxidation. Relatively recently, BP/SOHIO have developed catalytic materials for the direct ammoxidation of propane to acrylonitrile [4]. The most promising material reported had a rutile structure with Sb, V, Mo, and Al as the key elements [5–8].

* Corresponding author. Tel.: +1-513-556-0203; fax: +1-513-556-3473.
E-mail address: vadim.guliants@uc.edu (V.V. Guliants).

0920-5861/01/$ – see front matter
PII: S0920-5861(01)00333-9

Despite the promise of the results obtained and the numbers of patents obtained for mixed metal oxide catalysts, few fundamental studies have been undertaken on the nature of these materials [1,9]. The paucity of such publications is perhaps understandable given the complexity of the systems under study. Where the phase composition versus catalytic activity for binary and ternary systems may be thoroughly studied with relative ease, the study of a four-component catalyst is very time-consuming due to the large number of syntheses required using manual laboratory techniques [10].

A more recent patent, from Toagosei, described the use of Sb–Mo–V–Nb oxide materials for the production of acrylic acid from propane [11]. For the selective oxidation of propane at 400°C, this four-component system gave $S_{\text{acrylic acid}} = 39.5\%$ at 30.9% propane conversion. From the patent data it is apparent that little structural information is available for this very promising catalyst system. To help in understanding the behavior of a bulk catalyst, it is desirable to have thorough understanding of the chemistry of the solid state Sb–Mo–V–Nb catalysts as possible. Such structure–reactivity relationships are critical for the rational design of mixed metal oxides for propane oxidation. We therefore adopted this material as a model system for our study. This study explores the solid-state chemistry of two Sb–Mo–V–Nb catalysts with differing stoichiometries prepared using water-soluble precursors.

2. Experimental

Samples representative of the optimal catalyst composition [11] of this mixed metal oxide system, with two different molar ratios, were prepared in aqueous media: *Oxide 1* [1 Mo:1 V:0.4 Sb:0.4 Nb]; *Oxide 2* [3.3 Mo:1 V:0.4 Sb:0.4 Nb]. Soluble precursor materials were used in this study. Three stock solutions were prepared in deionized water: (i) V^{3+}/Sb^{5+} solution (Sb/V =0.4); (ii) $(NH_4)_6[Mo_7O_{24}]\cdot 4H_2O$ solution; (iii) $Nb_2(O_4C_2)_5/C_2O_4H_2$ solution. The ammonium metavanadate (99+%, Aldrich), antimony trioxide (99%, Aldrich), ammonium heptamolybdate (81–83 wt.% as MoO_3, Alfa Aesar) and oxalic acid (98%, Aldrich) were purchased commercially and used without further purification. Hydrated niobium oxide (80.3 wt.% Nb, Reference Metals Company) was also used without further purification.

2.1. Synthesis of $Nb_2(O_4C_2)_5\cdot xH_2O/C_2H_2O_4$

Oxalic acid (17.3 g, 0.192 mol) was dissolved in 200 ml of deionized water with stirring at 80°C in a 500 ml round bottomed flask fitted with a water condenser. Hydrated niobium oxide (80.3% Nb, 8.4 g, 0.073 mol) was added to this solution and the slurry heated with stirring at 80°C for 12 h, or until a clear solution was obtained. The solution was transferred to a 500 ml beaker and evaporated to dryness with stirring in air at 80°C (23.02 g, 0.073 mol Nb).

2.2. Preparation of V^{3+}/Sb^{5+} aqueous stock solution, solution A

Ammonium metavanadate (4.8 g, 4.1×10^{-2} mol V) was heated with stirring in 200 ml of deionized water in a 500 ml round-bottomed flask at 70°C until all was dissolved. The antimony trioxide (2.40 g, 1.64×10^{-2} mol Sb) was then added over a period of approximately 1 min. The mixture was then heated at reflux until all the antimony trioxide was dissolved, and the solution became dark brown (6–12 h).

2.3. Preparation of Mo^{6+} stock solution, solution B

Ammonium heptamolybdate (20 g, 82 wt.% MoO_3 = 0.114 mol Mo) was dissolved in 200 ml of deionized water with stirring.

2.4. Preparation of Nb^{5+} stock solution, solution C

Niobium oxalate/oxalic acid mixture (11.5 g, 3.63×10^{-2} mol Nb) dissolved in 100 ml of deionized water with stirring.

2.5. Synthesis of Oxide 1 (molar ratios 1 Mo:1 V:0.4 Sb:0.4 Nb)

Ammonium metavanadate (2.40 g, 20.37 mmol V) was heated to reflux under stirring in 200 ml of deionized water in a 250 ml round-bottomed flask until all was dissolved. To this solution were added antimony trioxide (1.2 g, 8.11 mmol Sb) and the solution refluxed for a further 12 h. A color change to brown was

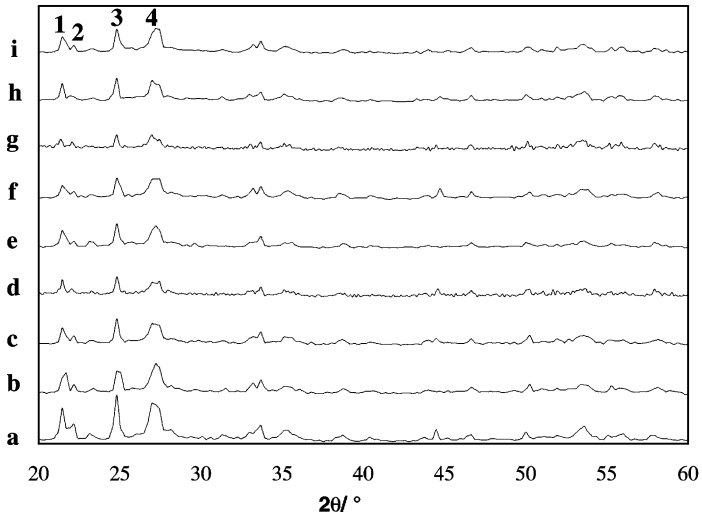

Fig. 1. X-ray powder diffraction patterns of *Oxide 1* prepared manually (a) and by automated methods (b–i); 1 = $Mo_6V_9O_{40}$, 2 = "$Mo_{0.6–0.71}V_{0.31–0.19}Nb_{0.08–0.04}O$", 3 = MoO_3, and 4 = $SbVO_4$.

noted. The solution was cooled to 60°C and ammonium molybdate (3.6 g, 67.8 mmol Mo) immediately followed by niobium oxalate (2.52 g, 8.04 mmol Nb) were added as powders. This mixture was stirred for a further 30 min at 60°C. The mixture was then reduced to a slurry over a period of 1–2 h at 120°C. The resultant slurry was calcined under flowing nitrogen for 4 h at 200°C followed by 8 h at 600°C.

2.6. Manual synthesis of Oxide 2 (molar ratios 3.3 Mo:1 V:0.4 Sb:0.4 Nb)

Ammonium metavanadate (2.40 g, 20.37 mmol V) was heated to reflux under stirring in 200 ml of deionized water in a 250 ml round-bottomed flask until all was in solution. To this solution were added antimony trioxide (1.2 g, 8.11 mmol Sb) and the solution was further refluxed for 12 h. A color change to brown was noted. The solution was cooled to 60°C and ammonium molybdate (11.88 g, 67.8 mmol Mo) immediately followed by niobium oxalate (2.52 g, 8.04 mmol Nb) were added as powders. This mixture was further stirred for 30 min at 60°C. The mixture was then reduced to a slurry over a period of 1–2 h at 120°C. The resultant slurry was calcined under flowing nitrogen for 4 h at 200°C followed by 8 h at 600°C.

The XRD spectra were recorded on a Phillips X-Pert PW1877 diffractometer using a Cu Kα radiation source. Micro-Raman measurements were recorded in a backscattering geometry, using a triple monochromator (ISA, Model T64000) using an [Ar^+] laser source emitting at λ = 514.5 nm at a power of 5 mW. The spectra were recorded using nine 9 s pulses with a spot size of 1–1.5 μm.

3. Results

3.1. X-ray diffraction

The data obtained for *Oxide 1* are shown in Fig. 1. The major reflections were observed at *d*-spacings of 4.12, 3.58, and 3.27 Å. Assignments of the mixture

Table 1
Assignment of phases present in *Oxide 1*

d-Spacing, Å (Manual synthesis)	Phase	JCPDS No.
4.12	$Mo_6V_9O_{40}$	[15]
4.00	"$Mo_{0.6–0.71}V_{0.31–0.19}Nb_{0.08–0.04}O$"	[1]
3.53	MoO_3	47-1081
3.37	Mo_4O_{11}	13-0142
3.28	$SbVO_4$	10-0600
2.98	Nb_2O_5	18-0910
2.69	$SbVO_4$	10-0600
2.52	$SbVO_4$	10-0600
2.32	$SbVO_4$	10-0600

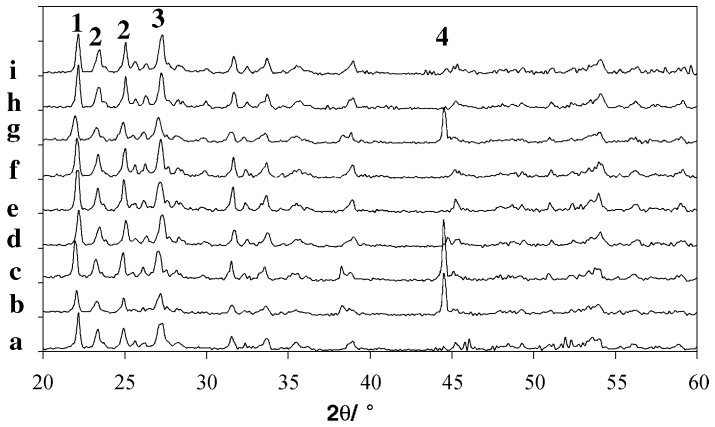

Fig. 2. X-ray powder diffraction patterns of *Oxide 2* prepared manually (a) and by automated methods (b-i); 1 = "$Mo_{0.6–0.71}V_{0.31–0.19}Nb_{0.08–0.04}O$", 2 = MoO_3, 3 = $SbVO_4$, and 4 = Sb_2O_3.

of the phases present are given in Table 1. The data obtained for *Oxide 2* are shown in Fig. 2. From the relative intensities of the peaks in the spectra it appeared that the material obtained from this synthesis was more crystalline than for *Oxide 1*. The major reflections were observed at *d*-spacings of 4.00, 3.58, and 3.27 Å. Assignments of the mixture of the phases present are given in Table 2.

3.2. Raman spectroscopy

Raman spectroscopy primarily provides information on the vibrational properties of a bulk oxide. Typically, Raman spectroscopy analyses to a depth of 1 μm into the surface of a solid [12]. Amorphous materials give poor Raman spectra. The rutile $SbVO_4$ phase was reported to be Raman inactive and is thus not observed in these spectra [13].

Table 2
Assignment of phases present in *Oxide 2*

d-Spacing, Å (Manual synthesis)	Phase	JCPDS No.
4.00	"$Mo_{0.6–0.71}V_{0.31–0.19}Nb_{0.08–0.04}O$"	[1]
3.80	MoO_3	47-1081
3.56	MoO_3	47-1081
3.46	Mo_4O_{11}	13-0142
3.28	$SbVO_4$	16-0600
3.25	$SbVO_4$	16-0600
3.14	Sb_2O_3	02-1283
2.83	$MoO_2{\cdot}Nb_2O_5$	18-0840
2.65	$SbVO_4$	16-0600
2.53	$SbVO_4$	16-0600
2.31	$SbVO_4$	16-0600
2.03	Sb_2O_3	02-1283

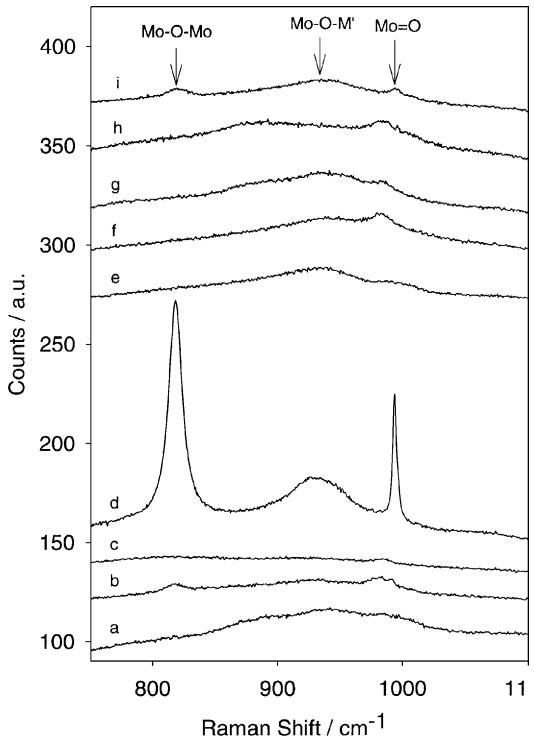

Fig. 3. Raman spectra of *Oxide 1* prepared manually (a) and by automated methods (b–i) with assignment of oxide phases present.

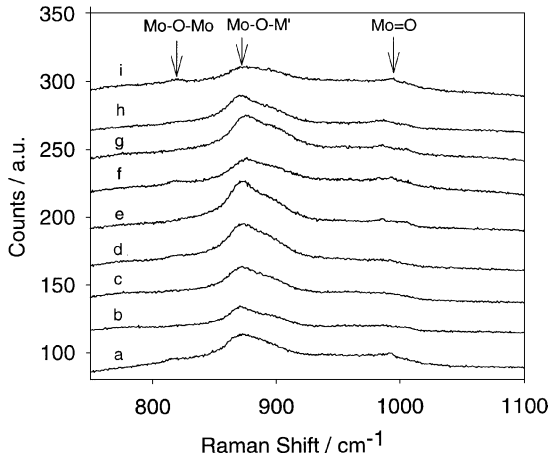

Fig. 4. Raman spectra of *Oxide 2* prepared manually (a) and by automated methods (b–i) with assignment of oxide phases present.

Analysis of *Oxide 1* by Raman spectroscopy, shown in Fig. 3, indicated that this material was only partially crystalline. No well-defined peaks were observed in the spectra. For the automated syntheses of *Oxide 2* we observed that one broad band at ca. 875 cm^{-1} dominated the Raman spectrum, Fig. 4.

The heterogeneity of these materials was illustrated by recording the Raman spectra at two other positions on the surface of *Oxide 2*, as shown in Fig. 5. Intense bands at 820 and 992 cm^{-1} were observed. Although

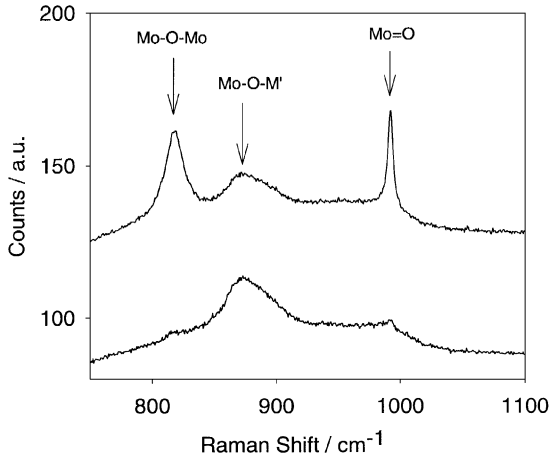

Fig. 5. Micro-Raman spectra of *Oxide 2* measured at different spots on the surface of the *Oxide 2*, with assignment of oxide phases present.

the laser spot size (1–1.5 μm) was greater than the individual crystallites present in the catalyst sample, different phase compositions were detected. It should be noted that the bands situated around 1000 cm^{-1} evidence the presence of domains of crystalline materials with terminal M=O bonds [14].

4. Discussion

Very little characterization data are available in the literature about the Sb–V–Mo–Nb oxides [11]. XRD analysis of materials prepared under a number of different reaction conditions demonstrated a change in intensity of the reflection at $2\Theta = 28.1^{\circ}$, which may be assigned to Sb_2O_3. The stoichiometric ratios used previously [11], indicate that almost all equimolar amounts of V and Sb were present in these syntheses (Mo:V:Sb:Nb = 1:0.3:0.25:0.1). Under this stoichiometric ratio it is possible that the formation of the rutile phase would not be thermodynamically favored, and unreacted Sb_2O_3 would remain in the final product.

Moreover, no details were given regarding the catalytically active phases present in this system [11]. Similarly, no indications were provided as to the role of the micro-crystalline phases present in this mixed oxide system. In our syntheses special care was taken to use stoichiometric ratios such that all Sb_2O_3 would be consumed in the formation of the catalytically active $SbVO_4$ rutile phase, i.e. V:Sb ratio 1 (*Oxide 1*, Mo:V:Sb:Nb = 1:1:0.4:0.4) (*Oxide 2*, Mo:V:Sb:Nb = 3.3:1:0.4:0.4). Thus, from the order of addition of the metal-containing precursors, it would appear that for both the syntheses of *Oxides 1* and *2* a possible initial step was the formation of $SbVO_4$. Once formed, an excess of molybdenum and a small amount of niobium were introduced into the solution.

For *Oxide 1*, preparation gave reflections at 4.12, 3.55, and 3.28 Å. Additionally, a minor phase was also observed, a reflection at 4.00 Å being noted. It has been shown, in a previous study of the solid state chemistry of the binary Mo–V oxide systems [15], that excess molybdenum oxide present during synthesis results in reduced vanadium-rich phases. Generally, if these binary mixtures contain between 18.5 and 33.3% V then the bulk mixed metal oxide contains two distinct mixed metal oxide phases, $Mo_4V_6O_{25}$

and $Mo_6V_9O_{40}$. The remaining fraction of the solid was shown to consist of orthorhombic or hexagonal MoO_3 phases. These binary Mo–V phases give strong reflections at 4.06 and 4.12 Å, respectively, in their XRD spectra, with the reflection for MoO_3 observed at 3.56 Å. However, in these pure phases, no reflection was observed at 4.00 Å.

Although the vanadium content in *Oxide 1* was higher in our synthesis (60 at.% after formation of $SbVO_4$), the reflection at 4.12 Å indicated that the formation of the binary phase $Mo_6V_9O_{40}$ still occurred. Further comparison of our results with the work of Thorsteinson et al. [1], on mixed Mo–V bulk oxides, indicated that the reflection at 4.00 Å was associated with Nb-containing mixed Mo–V bulk oxides. They identified this reflection as being probably due to a meta-stable layered defect phase of either $Mo_4V_6O_{25}$ or $Mo_6V_9O_{40}$, stabilized by the presence of Nb. The general formulae of these species were shown to be over the range $Mo_{0.61–0.77}V_{0.31–0.19}Nb_{0.08–0.04}$ [1]. Thus, the reflection at 4.00 Å indicated that small amounts of the Nb-stabilized defect phase, $Mo_{0.61–0.77}V_{0.31–0.19}Nb_{0.08–0.04}$ was obtained. There were two additional minor reflections observed at 3.37 and 2.98 Å, the former may be indexed to a partially reduced molybdenum cluster, Mo_4O_{11}, and the latter possibly due to the presence of unreacted Nb_2O_5. Thus, the major reflections observed may be indexed to $Mo_6V_9O_{40}$, MoO_3, and $SbVO_4$, respectively, and the minor $Mo_{0.61–0.77}V_{0.31–0.19}Nb_{0.08–0.04}$ phase.

In the synthesis of *Oxide 2*, the solid exhibited a strong reflection at 4.00 Å in the XRD pattern. Study of such materials [1] has indicated that the stoichiometric ratio of Mo/V/Nb for *Oxide 2* is in the optimal range for the synthesis of $Mo_{0.61–0.77}V_{0.31–0.19}Nb_{0.08–0.04}$, catalysts used for the selective oxidation of ethane to acetic acid [1]. The stabilization of the 4.00 Å defect phase perhaps provides geometry conducive to highly selective oxidation. In support of this, it has been previously reported that the catalysts that had the strongest reflections at 4.00 Å also had the highest activity for ethane oxidation [1]. The reflection at 3.57 Å indicated that the remainder of the molybdenum was in the form of crystalline polymeric MoO_3. Finally, the reflection at 3.27 Å may be attributable to the presence of $SbVO_4$ and/or α-Sb_2O_4. Given the stoichiometric ratios used (molar ratios of 3.3 Mo/1 V/0.4 Sb/0.4 Nb) one could argue that the former is the most likely.

Complementary data highlighting the heterogeneity present in samples of both *Oxide 1* and *Oxide 2* were obtained from the Raman spectroscopy studies. Although analysis of the spectra obtained for *Oxide 1* and *Oxide 2*, shown in Figs. 3 and 4, respectively, would seem to suggest that the material is essentially composed of disordered microcrystalline or amorphous phases. However, further micro-Raman experiments indicated that other more crystalline phases were also present and the presence of more crystalline or less disordered phases is illustrated in Fig. 5.

The spectra obtained for these solids gave bands at 820–932 and 992 cm^{-1}. The observed bands at 820 cm^{-1} have been previously associated with the Mo–O stretching mode of crystalline α-MoO_3 [14,16] and 992 cm^{-1} with the presence of isolated Mo species [15,17]. Raman bands in the region 860–940 cm^{-1} are generally characteristic of the M–O–M′ stretching mode in polycrystalline metal oxide phases [18]. A shift in the frequency of the Raman band to higher wavenumbers may be explained by substitution of one of the Mo atoms in the polycrystalline by a metal of lower atomic mass. Thus, for *Oxide 1* and *Oxide 2*, the bands at 932 and 873 cm^{-1}, respectively, probably indicate the presence of a crystalline Mo–O–V phase.

Micro-Raman analysis of two other locations on the surface of *Oxide 2*, as shown in Fig. 5, was also extremely informative. Conventional XRD and Raman techniques (which use a laser spot size of 80 μm) when applied to the same materials provide only the average phase composition of the bulk material. Micro-Raman clearly shows mixtures of phases at the micron level. Fig. 5a exhibits Raman absorption bands at 817, 874, and 994 cm^{-1} which, as discussed above, may be assigned to a mixture of α-MoO_3, a Mo=O-containing phase, and a crystalline Mo–O–V phase. In Fig. 5b the major crystalline phase observed was the Mo–O–V phase. We observed that the band at 992 cm^{-1} was very weak, suggesting that the phase associated with isolated molybdate species was either significantly disordered, or present in negligible quantity. Comparison of the spectra in Fig. 5, which illustrated the heterogeneity of the bulk material on the micro-scale shows the unique advantage of the micro-Raman technique.

From the above it is apparent that the optimal stoichiometric ratio (*Oxide 2*) gave both the $SbVO_4$ and $Mo_{0.61–0.77}V_{0.31–0.19}Nb_{0.08–0.04}$ phases as the major products formed. Thus, it would appear that a large

excess of Mo and a small amount of Nb encouraged the formation of the Nb stabilized reduced vanadium rich molybdate defect phase. The stoichiometric ratio of *Oxide 2* allowed for the preferential formation of the two phases that are thought to be the active phases for the selective oxidation of alkanes. From Raman spectroscopic results, we observed the heterogeneity of these phases. However, any enhancement of the catalytic activity for this material based on these observations remains to be explored.

5. Conclusions

This study explored the solid state chemistry of the four-component Mo–V–Sb–Nb oxide system. This system has been previously proposed as a selective catalyst for propane oxidation. Additional studies on $SbVO_4$, Sb–V–Nb–Al–O, and Mo–V–O systems have been published [1–3,19] and comparison with these available data has been made.

The solid state chemistry of this system has been studied, and has provided some critical insight into the possible catalytic function of these materials. From XRD data, all materials prepared contained the active phases necessary for the selective oxidation of light alkanes, namely $SbVO_4$ and $Mo_{0.61–0.77}V_{0.31–0.19}Nb_{0.08–0.04}$. From XRD studies the phase composition was shown to be different for the two stoichiometric ratios studied. Analysis of XRD data indicated that *Oxide* 2 gave a mixture of both $SbVO_4$ and $Mo_{0.61–0.77}V_{0.31–0.19}Nb_{0.08–0.04}$ as the major phases present. Although *Oxide 1* also contained both phases, the latter was present only as a minor phase. Thus it may be concluded that the stoichiometric ratio utilized for *Oxide 2* favors active catalyst preparation.

The micro-Raman techniques employed provided complementary data on the heterogeneity of these catalysts on the microscale. Whereas traditional Raman spectroscopic techniques utilize a laser spot size of ca. 80 μm, the micro-Raman technique allows us to probe the surface on a 1–1.5 μm scale. Thus, were the observed differences in the composition of the oxides prepared and individual phases present in the solid identified.

Future work will address catalytic activity of these materials as well as a study of the surface active sites of these materials through the utilization of an appropriate surface chemical probe such as MeOH or *i*-PrOH.

References

[1] E.M. Thorsteinson, T.P. Wilson, F.G. Young, P.H. Kasai, J. Catal. 52 (1978) 116.
[2] K. Ruth, R. Burch, R. Kieffer, J. Catal. 175 (1998) 27.
[3] R. Catani, G. Centi, F. Trifiro, R.K. Grasselli, Ind. Eng. Chem. Res. 31 (1992) 107.
[4] Newsletter, Appl. Catal. 67 (1990) N5.
[5] US Patents 4,746,641 (1988); 4,784,979 (1988); 4,788,317 (1988); 4,871,706 (1989); 4,877,764 (1989); 4,879,264 (1989); assigned to the Standard Oil Company, Ohio.
[6] G. Centi, P. Mazzoli, Catal. Today 28 (1996) 351.
[7] G. Centi, S. Perathoner, F. Trifiró, Appl. Catal. A 157 (1997) 143.
[8] G. Centi, P. Mazzoli, S. Perathoner, Appl. Catal. A 165 (1997) 273.
[9] G. Centi, D. Pesheva, F. Trifiró, Appl. Catal. 33 (1987) 343.
[10] J. Klein, C.W. Lehman, H.W. Schmidt, W.F. Maier, Angew. Chem. Int. Edit. 37 (1998) 3369.
[11] M. Takahashi, X. Tu, T. Hirose, M. Ishii, US Patent 5,994,580 (1999); assigned to Toagosei Co., Ltd., Japan.
[12] J.M. Stencel, Raman Spectroscopy for Catalysis, van Nostrand Reinhold, New York, 1990.
[13] J. Nilsson, A.R. Landa-Cánovas, S. Hansen, A. Andersson, J. Catal. 186 (1999) 442.
[14] N.C. Ramani, D.L. Sullivan, J.G. Ekerdt, J.-M. Jehng, I.E. Wachs, J. Catal. 176 (1998) 143.
[15] R.H. Munch, E.D. Pierron, J. Catal. 3 (1964) 406.
[16] D.S. Kim, I.E. Wachs, K. Segewa, J. Catal. 146 (1994) 248.
[17] J.P. Dunn, H.G. Stenger Jr., I.E. Wachs, Catal. Today 53 (1999) 543.
[18] C.C. Williams, J.G. Ekerdt, J.-M. Jehng, F.D. Hardcastle, A.M. Turek, I.E. Wachs, J. Phys. Chem. 95 (1991) 8781.
[19] R.K. Grasselli, Catal. Today 49 (2000) 141.